AUTOMATIC FEATURE EXTRACTION AND CLASSIFICATION OF SURFACE DEFECTS IN CONTINUOUS CASTING

Qingyu Yang and Jionghua Jin
Department of Industrial and Operations Engineering
University of Michigan
Ann Arbor, Michigan

Tzyy-Shuh Chang
OG Technologies, Inc.
Ann Arbor, Michigan

KEYWORDS

Continuous casting, process monitoring, feature extraction, classification method

ABSTRACT

The problem of surface defects is a major quality concern in continuous casting. Although there exist methods in the literature to effectively detect surface defects, most are limited to specific defect types, and there is a paucity of research for classification of various defects. This paper presents a methodology for online detection and classification of surface defects in continuous casting using vision-based sensing technology. First, a two-stage algorithm is proposed to effectively extract potential surface defect regions from the noisy background. Then, the potential surface defects are classified into different categories using a newly developed classification method. The proposed methods are implemented and validated using data collected from a real world continuous casting process.

INTRODUCTION

Continuous casting is a modern manufacturing process that converts ingot, process scraps, or virgin metal (or a combination of these) by melting and casting to produce a "semi finished" section (Yu 2001). Surface defects are critical quality concerns in continuous casting because the defects on the surface of steel billets have severely degraded their appearance and quality. Detecting the surface defect at an early stage, therefore, can highly reduce the re-melting for the defective product, and thus, reduce the energy and production costs.

In recent years, progress has been made for automatic surface defect detection in casting processes. Kitagawa et al. (1981) proposed a method to detect the surface defects using infrared scanning camera. Ignacio et al. (2009) developed an online inspection system based on conoscopic holography measurement technology, which can detect surface defect of hot steel slabs under high temperatures up to 900ºC. Ershun et al. (2009) developed a method of online detection of bleeder defect in continuous casting using a vision sensor system.

Although these methods can effectively detect defects in casting processes, most are limited to specific defect types, and there is a paucity of research for classification of various defects. In continuous casting, surface defects can be classified into different categories (e.g., crags, bleeders, slag pits, cracks, and oscillation marks). Each type of surface defect often relates to some specific process problems, such as metal level fluctuation, mold thermal response, lubrication, or steel carbon content. Therefore, accurately classifying surface defects is important for identifying the root causes of surface defects, helps to expedite the process correction decision, as well as to reduce the process downtime and manufacturing cost.

In this paper, an on-line surface defect detection and classification methodology is developed for continuous casting. The paper

begins with an introduction, then describes a vision-based inspection system applied in continuous casting. Next, details of the methodology are presented, and the experimental results are shown, followed by conclusions.

VISION SENSOR SYSTEM APPLIED IN A CONTINUOUS CASTING PROCESS

In recent years, with the advancement of vision technology, vision-based inspection systems have been successfully applied in the hot deforming processes, (e.g,, rolling processes and continuous casting), to collect high quality sensing images of product surface under high temperatures up to 1450˚C (Ershun et al., 2009; Li et al., 2007; Yang et al., 2009). Figure 1 shows the vision sensing system installed in a continuous billet caster before the product is fully solidified; Figure 2 illustrates a portion of the sensing images; and Figure 3 highlights different categories of surface defects.

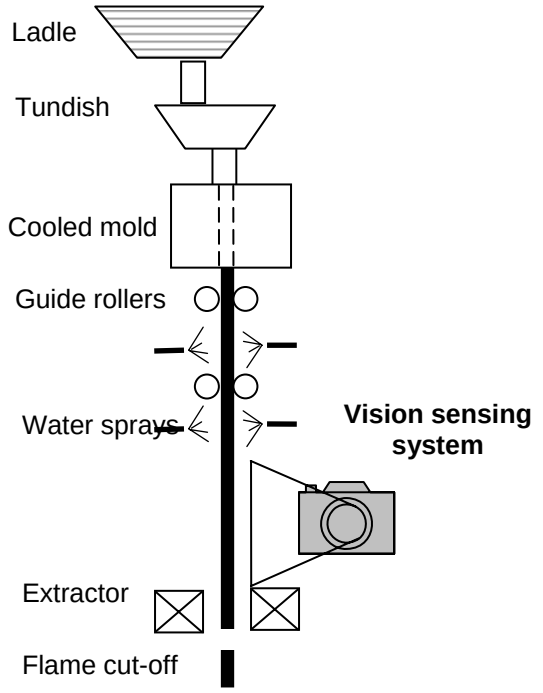

FIGURE 1. THE VISION SENSING SYSTEM APPLIED IN A CONTINUOUS CASTING PROCESS

In the literature (Li et al., 2006, Yang et al., 2009), methods have been developed for detecting and classifying surface defects in hot rolling processes using sensing images. Those

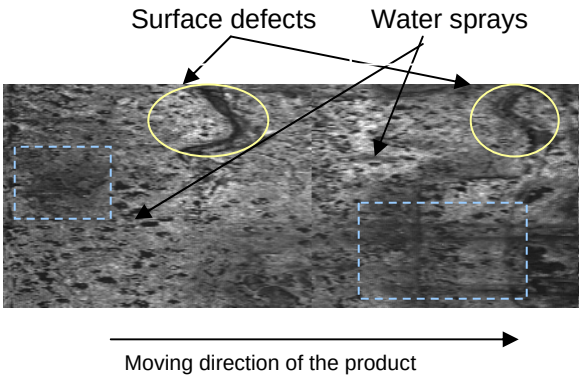

FIGURE 2. A PORTION OF REAL TIME SENSING IMAGE IN A CONTINUOUS CASTING PROCESS (92mm*144mm)

methods, however, cannot be directly applied for continuous casting. There are a few major challenges of analyzing images in casting processes. First, the sensing images for continuous casting have a lower signal to noise ratio. The noise may arise from different sources at multiple scales, such as vaporized steam spot, long strips of water sprays, and unavoidable oxidized substances. Second, in continuous casting, shapes of the surface defects are complex and the background texture is extremely complicated. Finally, the image data in continuous casting has a huge volume, making existing methods inappropriate for online detection and classification under time constraints.

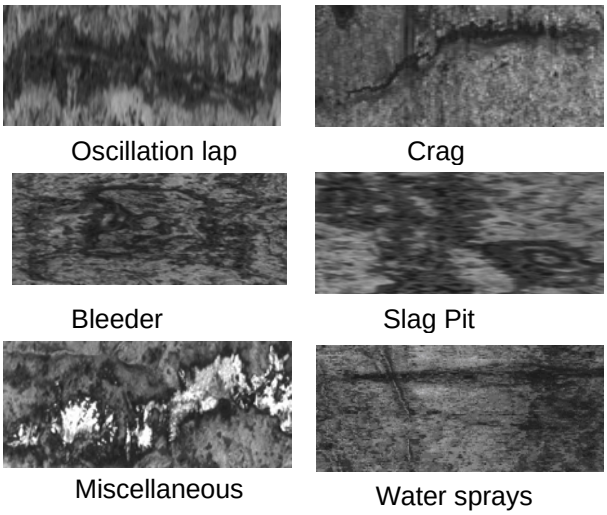

FIGURE 3. EXAMPLES OF VARIOUS SURFACE DEFECTS (22mm*28mm)

METHODOLOGY

As shown in Figure 4, the proposed methodology consists of three fundamental steps, including defect region extraction, feature generation, and surface defect classification.

Two-stage defect region extraction method

The first step of the proposed method is to detect and extract surface defect regions from the complex background. As illustrated in Figure 2, the sensing image has a low signal to noise ratio and surface defects generally have very complex shapes. Directly applying the traditional region detection methods, therefore, cannot generate accurate results under the time constraints. For example, the active contour based region segmentation method for an image of size 1MB can take minutes for the segmentation process (Svoboda et al., 2008). The size of typical images in continuous casting can reach over 100 MB for a one-minute time interval. For such large size images, most region detection algorithms are unrealistic for online analysis.

A two-stage method is proposed in the paper to effectively extract regions of potential surface defects. The first stage focuses on quickly identifying the location of the possible defects. The exact region of the defects is further extracted by using texture analysis at the second stage.

At the first stage, the monitoring system identifies rectangular regions that contain potential surface defects. To quickly identify the defect location, a 2-dimensional rectangular window with a given size is used to go through the whole picture sequence. The size of the rectangular window is chosen so that all possible defects could be contained in the window.

As illustrated in Figure 3, compared to the background, surface defects have either a lower gray level, (e.g. crag, bleeder), or a higher gray level, (e.g, miscellaneous). Therefore, by comparing the average grey level of the pixels in the window to the background level (determined by an upper and a lower threshold), the rectangular regions that contain potential surface defect can be obtained. Figure 5 (a) illustrates a detected rectangular region that contains a surface defect in sensing images and Figure 5(b) shows the corresponding defect in the final product. The detected surface defect region will be used an example throughout the paper to illustrate the developed methods.

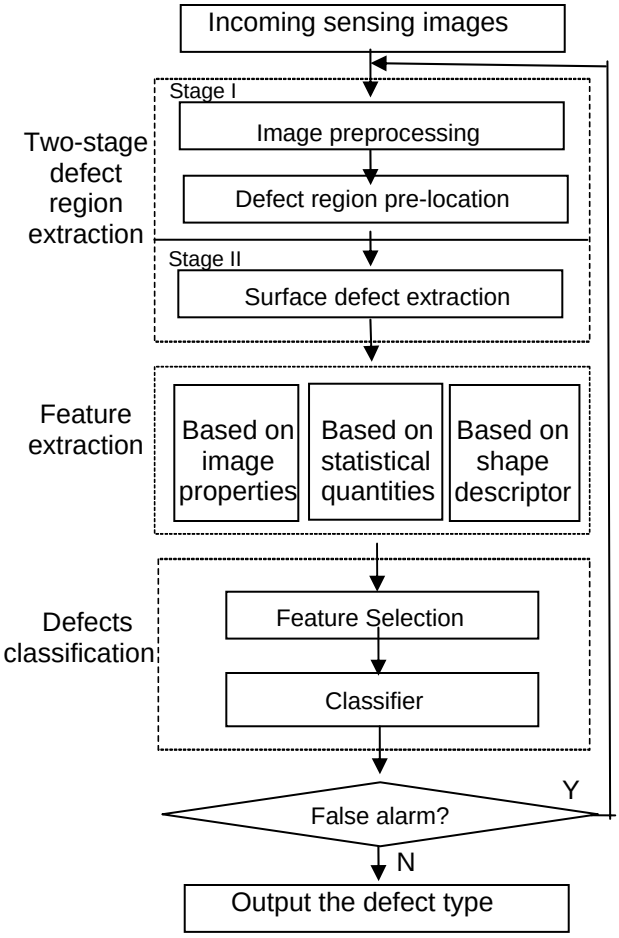

FIGURE 4. METHODOLOGY OF DETECTION AND CLASSIFICATION OF SURFACE DEFECTS IN CONTINUOUS CASTING

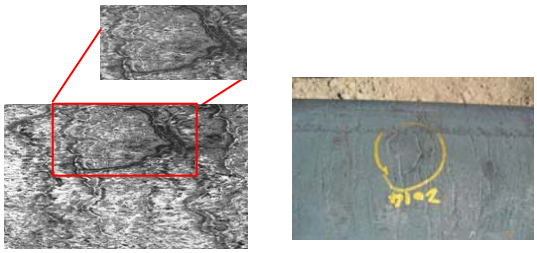

(a) (b)

FIGURE 5. (a) IDENTIFICAONT OF RECANTIGULAR REGIONS THAT CONTAIN POTENTICAL SURFACE DEFECTS (82mm*50mm) (b) SURFACE DEFECT DETECTED IN THE PRODUCT OFF-LINE

At the second stage, surface defects are extracted from the rectangle regions identified in the first stage. Figure 3 demonstrates that the intricate surface defect region is mingled with the complex background. Furthermore, the grey levels of both the background and the surface defects may change significantly when billets are made from different materials. As a result, region extraction methods based on grey level are not effective for detecting the exact region of various surface defects. In this research, a texture-based method is developed to extract regions of complex surface defects. As shown in Figure 6, the developed algorithm includes three steps: texture analysis, noise filtering, and image dilate.

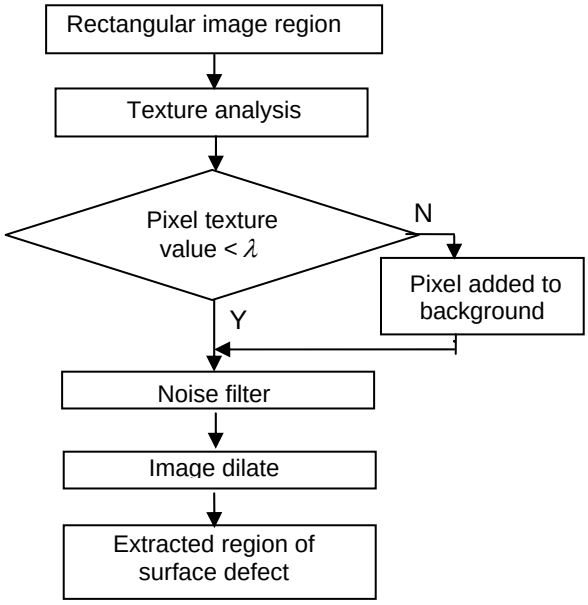

FIGURE 6. ALGORITHM TO EXTRACT SURFACE DEFECT REGION BASED ON TEXTUTE PROPERTIES

Texture analysis Although the regions of surface defects have large variation of grey levels, they follow specific patterns, which are defined as the image textures. In this research, the Standard Deviation (STD) Filter (Svoboda et al., 2008), widely used in the literature to capture the texture information, is applied to calculate the texture value of each pixel in the rectangular regions. The STD filter calculates the local standard deviation of the image intensity within a moving window, and the texture value of the pixel at point (*i*, *j*), denoted as $T(i,j)$ is obtained as follows:

$$T(i,j)=\sqrt{\frac{\sum_{p=-s}^{s}\sum_{q=-s}^{s}\left[G(i+p,j+p)-M\right]^2}{(2s+1)^2-1}} \quad (1)$$

$G(i,j)$ represents the intensity level at point (*i*,*j*), *s* represents the size of the moving window; and *M* is the mean of the intensity of all the pixels within the moving window. *M* is calculated as.

$$M=\frac{\sum_{p=-s}^{s}\sum_{q=-s}^{s}G(i+p,j+p)}{2s+1} \quad (2)$$

Then, by comparing the texture values, denoted by $T(i,j)$, of each pixels to a threshold λ, the regions of surface defects are extracted as follows:

$$I(i,j)=\begin{cases}1 & \text{if } T(i,j)<\lambda\\ 0 & o.w.\end{cases} \quad (3)$$

$I(i,j)$ is an identification function. Pixel (i,j) will be considered within the region of surface defects if $I(i,j)=1$; otherwise, it belongs to the background.

In general, the threshold λ in equation (3) may change with different backgrounds. In this paper, threshold λ is adaptively obtained using the following iterative algorithm.

Step 1: Initially set λ as mean of $T(i,j)$, i.e., $\lambda^{(0)}=E(T(i,j))$.

Step 2: Assign each pixel either to surface defects or background based on (3).

Step 3: At the k^{th} iteration, for pixels belonging to surface defects and those belonging to background, calculate the mean of texture values, respectively.

$$\mu_d=E(T(i,j)) \quad \text{for } I(i,j)=1$$
$$\mu_b=E(T(i,j)) \quad \text{for } I(i,j)=0$$

Step 4: Set $\lambda^{(k)}=\frac{\mu_d+\mu_b}{2}$, if $\lambda^{(k)}=\lambda^{(k-1)}$, the optimal threshold is obtained as $\lambda^{(k)}$; otherwise go to Step 2.

Noise filtering As mentioned previously, sensing images generally contain various noises, which are introduced into the extracted surface

defect regions. As an illustration, Figure 7(a) shows the extracted surface defect regions for Figure 5. Compared to surface defect regions, the noises have much smaller region sizes. Therefore, regions having sizes smaller than a threshold α are treated as noises. The noised filtered image is denoted by I' in the remaining paper. As an example, Figure 7(b) shows the image with noise filtered for Figure 7(a).

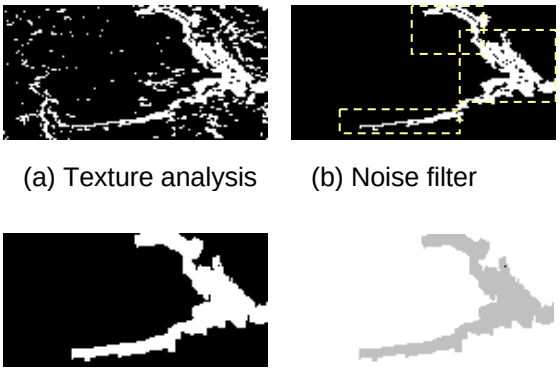

(a) Texture analysis (b) Noise filter

(c) Image dilate (d) Defect region

FIGURE 7. EXTACTION OF SURFACE DEFECTS FROM THE RECTANGULAR REGION (40mm*28mm)

Image Dilate The regions of surface defects may have been disconnected. Therefore, dilation operation is applied to link separated regions. Dilation is one of the two basic operators of mathematical morphology used to gradually enlarge the boundaries of regions. The dilation operation for binary image I' that contains separate defect regions is described as follows:

Suppose that $W = \{w_1, w_2, ...\}, w_i = (x_i, y_j)$, is the set of coordinates in I' such that $I'(w_i) = 1$, and K is the set of coordinates for the structuring element (an example of K is illustrated in Figure 8a). Let K_{w_i} denote the translation of K so that its origin is at w_i . Then the dilation of W by K would simply be the set of all points x such that the intersection of K_{w_i} and W is non-empty. For example, when selecting the structuring element K as illustrated in Figure 8(a), the dilation result for a 2×2 rectangle is illustrated in Figure 8(b).

In this research, the binary image I' is recursively dilated until all the defect regions are connected. The connected region, denoted by I'' , represents the potential surface defect. Figure 7(c) shows the dilated image of Figure 7(b), and the corresponding surfaced defect region is illustrated in Figure 7(d).

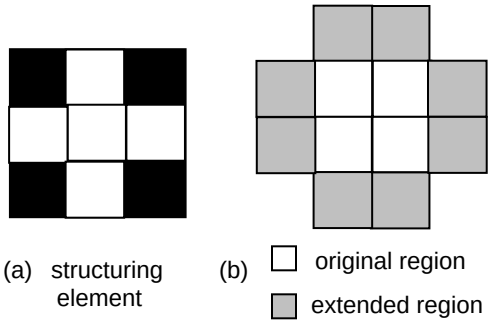

(a) structuring element (b)

FIGURE 8. STRUCTURING ELEMENT SELECTION AND ITS APPLICATION FOR A 2*2 RECTANGULAR REGION

Feature generation

After obtaining the surface defects region, a number of features are generated based on image properties, statistical quantities, and shape descriptors. Due to space limitation, this paper focuses solely on feature extraction based on the shape descriptors of identified surface defect regions.

In general, there are two types of shape descriptors, boundary-based and region-based shape descriptors. Because surface defects in the continuous casting generally have complex shapes, region-based shape descriptors are more reliable than boundary-based shape descriptors, since they rely not only on the contour pixels, but also on all pixels constituting the shapes.

Different types of surface defect may have different shape characteristics. For example, surface defects crag and false alarm water spray generally appear in the strip regions, while surface defect bleeder and slag pit tend to have ellipsoid regions. As a result, this research proposed that a feature f , capturing this shape property, distinguishes those two groups of surface defects, with f defined as follows.

$$f = \frac{d_1}{d_2} \qquad (4)$$

where d_1 indicates the length of the minor axis of the ellipse that has the same normalized second central moments as the region, and d_2

presents the length of the major axis of the same ellipse. Similar features are extracted for describing the shape of specific, or a set of, surface defects.

In this study other than features obtained based on vision appearance of the specific surface defects, features capturing the common characterizes of object shape are also derived based on Zernike moments (Khotanzad and Hong, 1990). These features are rotation invariant and robust to noise for describing the shapes patterns.

Surface Defects Classification

Based on the extracted features, termed "feature pool," and defined as **F**, different types of surface defects as well as the false alarms are further identified.

Classification method HWSVM In the author's previous work (Yang et al., 2009), a two-step classification method, called HWSVM, was developed to classify surface defects in hot rolling processes. In the first step, a Genetic Algorithm (GA) was developed to eliminate the redundant features and select a subset of the optimal features $\mathbf{F}_s$ from the feature pool **F**, $\mathbf{F}_s \subseteq \mathbf{F}$. Secondly, a hierarchical weighted Support Vector Machine (HWSVM) classifier was proposed to improve the classification accuracy. The main idea of the hierarchical classifier was to classify defects at two levels. At the higher level, surface defect classes that were difficult to be distinguished were automatically identified and grouped as mixed classes. Then, the mixed classes, as well as other defect types, were classified using a weighted Support Vector Machine (WSVM). At the lower level, the defect types in mixed classes were further classified using separate classifiers (also WSVMs).

Classification method AHWSVM In the HWSVM classifier, the feature set $\mathbf{F}_s$ obtained from the feature selection procedure is used for all the WSVMs in the hierarch classifier. This strategy, however, is not effective in continuous casting. In continuous casting, the sample numbers of all classes, (e.g., C_2 and C_3), in a mixed class M_1 could be small. Therefore, features that can efficiently distinguish classes C_2 and C_3 are not selected in $\mathbf{F}_s$ since improvement of the classification accuracy for classes C_2 and C_3 would only contribute small increment of the overall classification accuracy.

An improve classification method, called Adaptive HWSVM (AHWSVM) is developed in this paper to adaptively select different feature sets, (i.e., $\mathbf{F}_i$, $\mathbf{F}_i \subseteq \mathbf{F}$,) for the i^{th} WSVM in the hierarchical classifier. The structure of the AHWSVM is illustrated in Figure 9.

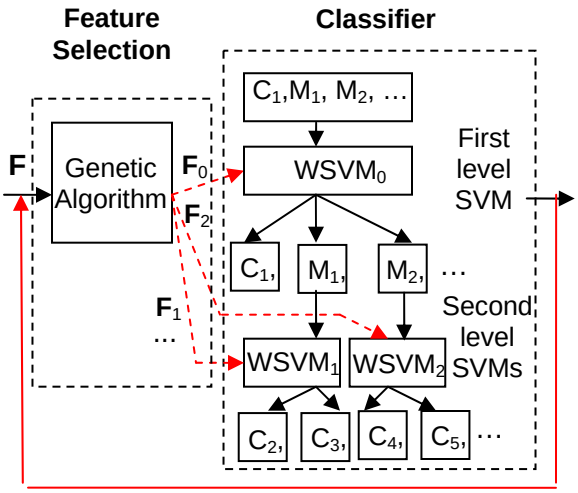

$WSVM_i$: the i^{th} weighted Support Vector Machine **F**: Feature pool; $\mathbf{F}_i$:the i^{th} subset of features selected for $WSVM_i$; C_i**:** the i^{th} class; M_i**:** the i^{th} mixed class

Figure 9. STRUCTURE OF THE AHWSVM CLASSIFICATION METHOD

The detailed procedure of AHWSVM is given as follows:

Step 1: A subset of the optimal features $\mathbf{F}_s$ is selected from feature pool **F** based on GA method (Yang et al., 2009).

Step 2: Classes that are difficult to be distinguished are automatically detected and combined as mixed classes, denoted as M_1, M_2,…(Yang et al., 2009).

Step 3: A new subset of the optimal features $\mathbf{F}_0$ is selected from feature pool **F** using the GA method. At the high level of the hierarchical classifier, based on feature set $\mathbf{F}_0$, the mixed classes, as well as other defect types are

classified using a weighted Support Vector Machine (WSVM).

Step 4: At the low level of the hierarchical classifier, new subsets of the optimal features $\mathbf{F}_k$ are selected from feature pool **F** for the k^{th} WSVM, based on which defect types in the k^{th} mixed classes are further classified.

CASE STUDY

In this case study, sensing images are taken from a continuous casting process in which billets with diameters of 200mm move at an average velocity of 6 cm/s. The image data consists of 300 images containing 350 defect regions. After applying the developed algorithm with the rectangular window size chosen as 380*400, 712 potential defect regions are identified, including all of the real defect regions.

The potential defect regions are further categorized into eight classes. The first five classes are different types of surface defects and the last two classes are false alarms. Because the false alarm "water spray" has a very different shape from all other false alarms, it is treated as a separate class to improve the classification accuracy. Table 1 shows the name of eight classes and the corresponding sample sizes. The samples are randomly divided into the training data set and testing data set. For each type of surface defects, the number of the samples assigned in the training data set is twice as that in the testing data set.

TABLE 1. CLASSES OF SURFACE DEFECTS.

Class Index	Types of Surface Defects	Number of Samples
1	Bleeder	74
2	Oscillation lap	142
3	Crack	44
4	Miscellaneous	48
5	Slag pit	42
6	False alarm 1 (water spray)	80
7	False alarm 2 (other type)	282

In the feature extraction process, 85 features are extracted for each sample image. These features are used as the input of the classification method.

Comparison of classification performance of HWSVM and AHWSVM

In this subsection, the performance of the HWSVM method and the AHWSVM method are compared. At the first level of the hierarchical classifier, class 1 and class 5 are identified as physically similar, and thus are mixed as a mixed class M_1. Similarly, classes 3, 4, and 6 are mixed as another mixed class (i.e., M_2). As a result, 3 WSVMs exist in the hierarchical classifier, including one WSVM at the first level and two WSVMs to classify classes in M_1 and M_2, respectively.

When applying the HWSVM for classification, 63 features are selected from the feature pool and used for all three WSVMs. The overall classification accuracy of HWSVM is 85%. Table 2 lists the classification accuracies for each individual class. Table 2, illustrates that the classification accuracy for class 1 and class 5 are much lower than that of other classes.

TABLE 2. CLASSIFICATION RESULT FOR HWSVM.

Class Index	Types of Surface Defects	Accuracy (%)
1	Bleeder	76
2	Oscillation lap	86
3	Crack	92
4	Miscellaneous	99
5	Slag pit	82
6	False alarm 1	84
7	False alarm 2	86

For the AHWSVM method, different sets of features are selected separately for three WSVMs in the classifier. Table 3 enlists the numbers of features selected for each WSVMs. The overall classification accuracy when applying AHWSVM is 87%. Table 4 shows the classification accuracies for each class, highlighting how the AHWSVM method not only increases the overall classification accuracy, but also greatly improves the classification accuracy for classes 1 and 5.

In conclusion, the developed methods can effectively detect and classify different types of surface defects in continuous casting.

TABLE 3. NUMBER OF FEATURES SELECTED FOR WSVMs WHEN APPLYING AHWSVM.

WSVM	Identified classes	Number of features
1	M_1,M_2, classes 2 and 7	52
2	classes 1 and 5	39
3	classes 3, 4, and 6	59

TABLE 4. CLASSIFICATION RESULT FOR HWSVM.

Class Index	Types of Surface Defects	Accuracy (%)
1	Bleeder	90
2	Oscillation lap	86
3	Crack	94
4	Miscellaneous	99
5	Slag pit	96
6	False alarm 1	86
7	False alarm 2	84

Summary

A monitoring system framework is proposed in the paper to detect and classify different types of surface defects in continuous casting under high temperatures. The new algorithms have been validated through real world production data. The results show that the proposed algorithms can effectively and efficiently detect the surface defects in the continuous casting with respect to different materials and operational conditions. In addition, the developed method satisfied time constraints for the online purpose. Future work includes further improving the classification accuracy, and developing models to identify the root causes of the surface defects based on the monitoring results.

ACKNOWLEDGEMENTS

This research is jointly supported by the NSF DMI F0541750 and 21st Century Jobs Fund F015886. The authors would also like to thank OG Technologies, Inc. for the valuable supports to this research.

REFERENCES

Ershun Pan, Ye, L., Shi, J., and Chang, T.-S. (2009). "On-line bleeds detection in continuous casting processes using engineering-driven rule-based algorithm." *Journal of Manufacturing Science and Engineering*, accepted.

Ignacio Alvarez, Jorge Marinab, Jose Maria Enguitaa, Cesar Fragac, and Garciab, R. (2009). "Industrial on-line surface defects detection in continuous casting hot." *Optical Measurement Systems for Industrial Inspection VI*, Vol. 7389, pp. 1-9.

Khotanzad, A., and Hong, Y. H. (1990). "Invariant image recognition by Zernike moments." *IEEE transactions on pattern analysis and machine intelligence*, Vol. 12, pp. 489-497.

Kitagawa, H., Fujii, A., Miyake, S., and Kurita, K. (1981). "An Automatic Surface Defect Detection System for Hot Ingot Casting Slabs Using an Infrared Scanning Camera and Image Processors." *Transactions of the Iron and Steel Institute of Japan*, Vol. 21, pp. 201-210.

Li, J., Shi, J., and Chang, T. S. (2007). "On-line seam detection in rolling processes using snake projection and discrete wavelet transform." *Journal of Manufacturing Science and Engineering*, Vol. 129, pp. 926-933.

Li, X., Tso, S. K., Guan, X. P., and Huang, Q. (2006). "Improving automatic detection of defects in castings by applying wavelet technique." *IEEE Transactions on Industrial Electronics*, Vol. 53, pp.1927-1934.

Svoboda, T., Kybic, J., and Hlavac, V. (2008). *Image processing, analysis, and machine vision : a Matlab companion*, Thomson Learning, Toronto, Ont.

Yang, Q., Li, Q., Jin, J., and Chang, T.-S. (2009). "Online Classification of Surface Defects in Hot Rolling Processes." Transactions of NAMRI/SME, Vol. 37, pp. 371-378.

Yu, K. O. (2001). *Modeling for casting and solidification processing*, CRC press, Boca Raton, FL.